Iranian Journal of Geophysics, Vol 17 No 3, 2023, Page 45 – 63 (Review Article)
DOI: 10.30499/IJG.2023.366469.1466

A review of Shallow Water Flows (SWF) and evaluation of this problem by 3D seismic data in the South Caspian Basin, Iran

Zohre Noorbakhsh Razmi,[1] Naser Hafezi Moghaddas,[2*] Hossein Sadeghi,[3] Sayyed Reza Moussavi Harami,[4] and Naser Keshavarz Farajkhah[5]

[1] *Ph.D. student, Department of Geology, Faculty of Science, Ferdowsi University of Mashhad, Mashhad, Iran*
[2] *Professor, Department of Geology, Faculty of Science, Ferdowsi University of Mashhad, Mashhad, Iran*
[3] *Associate Professor, Department of Geology, Faculty of Science, Ferdowsi University of Mashhad, Mashhad, Iran*
[4] *Professor,Department of Geology, Faculty of Science, Ferdowsi University of Mashhad, Mashhad, Iran*
[5] *Assistant Professor,Research Institute of Petroleum Industry (RIPI), Iran*

(Received: 22 October 2022, Accepted: 21 February 2023)

Abstract

Shallow Water Flow (SWF) is a type of geohazard in hydrocarbon exploration in deep-water basins. This problem occurs in deep-water basins with high sedimentation rates. When the drill hits over-pressured layers below the seabed, large volumes of water and sand flow along the wellbore and ultimately, loss of well integrity may occur. This is the first study to review the literature on predicting SWF predrilling from different aspects comprehensively. We also evaluate the SWF problem in the channel by using 3D seismic data in the South Caspian Basin (SCB) as an example of a deep-water basin prone to SWF geohazard. The results of the literature show that geological settings with rapid subsidence are more likely to be associated with SWF. Pleistocene low-stand sands, channels, slumps, and chaotic zones are more prone to SWF. Compaction disequilibrium, differential compaction, and hyperpressure are the mechanisms of SWF. The most important quantitative criteria for identifying SWF environments are Vp/Vs and Poisson's ratios, P-impedance (AI), and S-impedance (SI). Post-stack and pre-stack inversion, seismic stratigraphy, seismic attributes, and geopressure prediction are the most important techniques for evaluating SWF. The results of post-stack inversion including low impedance zones and AI<3150 ((m/s).(g/cc)), show SWF problem in the central and eastern parts of the buried channel in the SCB. The review findings provide a comprehensive understanding of SWF geohazard in deep-water basins. As recommended in this review, further review research should be done to stabilize shallow water flow zone during the drilling operation.

Keywords: Shallow Water Flow (SWF), Caspian Sea, geohazard, overpressure zone, rapid subsidence

*Corresponding author: nhafezi@um.ac.ir

1 Introduction

Shallow drilling hazard evaluation consists of geological and geophysical parameters review to reduce the problems that affect drilling safety. According to McConnell et al. (2012), three critical issues could affect the safety of shallow drilling: shallow water flows (SWF), gas hydrate and gas sands. Shallow water flows are the most common and crucial shallow drilling hazard in deep-water basins (McConnell et al., 2012). These sandy sediments are formed in deep-water basins with high sedimentation rates and lack of consolidation and drainage conditions. As soon as the drill reaches SWF sands in submarine drilling, the large volume of overpressure sands flows to the well and may destroy the platform, facilities and drilling rigs. Moreover, it may cause financial loss.

The first SWF identification was reported in 1985 (Lu et al., 2005). Some researchers have represented the mechanisms (Alberty et al., 1999; Huffman and Castagna, 2001), geological setting and the criteria of SWF evaluation (Ostermeier et al., 2002; Lu et al., 2005; Dutta et al., 2010, 2021). Today, various methods have been developed for the identification of SWF sands, such as Huffman and Castagna (2001), Mallick and Dutta (2002), Dutta et al., (2010, 2021) and Gherasim et al. (2015). These methods are used individually or in combination together. Many researchers have focused on predicting the SWF phenomena using 2D and 3D seismic data (Huffman and Castagna, 2001; Lu et al., 2005; Dutta et al., 2010; Zhang et al., 2018), log types (Ostermeier et al., 2002; Gherasim et al., 2015) and in situ measurements (Ostermeier et al., 2002). Several attempts have been made to obtain Vp/Vs anomalies for the detection of SWF zones by pre-stack inversion (Huffman and Castagna, 2001; Mallick and Dutta, 2002; Dutta et al., 2010). Huffman and Castagna (2001) detected the potential of SWF sands by using multicomponent seismic data and an inverted Vp/Vs ratio. Due to the cost implications of multicomponent seismic data (Lu et al., 2005), various studies have used pre-stack inversion of conventional 3D seismic data to estimate quantitative parameters (Vp/Vs and Poisson's ratio) (Mallick and Dutta, 2002; Lu et al., 2005, Dutta et al., 2021). Although SWF is among the foremost common and high-risk geohazards in deep water around the world and is widely used in oil exploration studies in deep-water basins, no review paper has been presented about this geohazard yet. In this study, the qualitative research data were collected from the different published papers about predicting SWF problem predrilling. These studies clarify ambiguous concepts and enhance our knowledge about SWF. This is the first study to review the different aspects of SWF phenomena, including mechanism, damages, impacts on drilling wells and their facilities, geological prone areas and identification and prediction methods integrately.

This paper is divided into three parts including method (section 2), results and discussion (section 3), and evaluation of SWF problem in the South Caspian Basin (SCB) as a case study (section 4). The section 3 contains geological setting, mechanisms, identification criteria, and study methods of SWF sands. The section 4 includes geology of SCB, data and method, and results and discussion. In this section, the criteria for identifying the SWF within the SCB is examined and the SWF problem is evaluated by 3D seismic data and post-stack seismic inversion in this basin. The South Caspian Basin has been extensively studied for oil exploration and scientific research. It is one of the areas prone to SWF and has all characteristics associated with the formation of this geohazard.

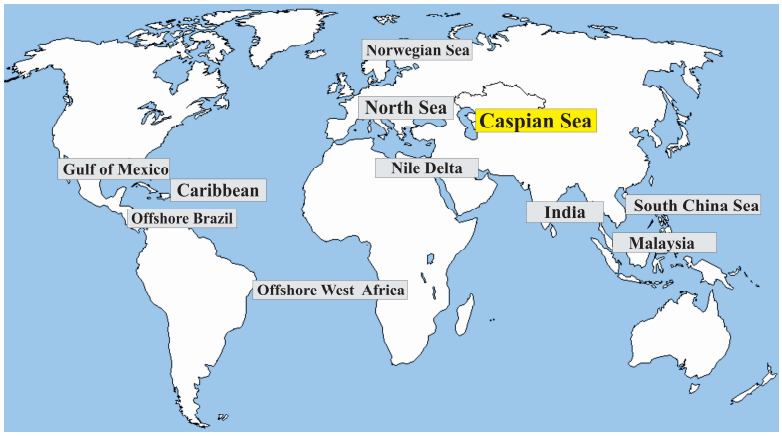

Figure 1. Known areas with SWF potential (Modified after Ostermeier et al., 2002).

Table 1. Sedimentary features associated with the SWF

Stratigraphic Feature/Facies	Authors
Canyon	(Ostermeier et al., 2002; Zhang et al., 2018)
Channel	(Ostermeier et al., 2002; Lu et al., 2005; Dutta et al., 2010; Wu et al., 2018; Zhang et al., 2018)
Slump, Debris flow	(McConnell, 2000; Lu et al., 2005; Zhang et al., 2018)
Turbidite Sands	(Dutta et al., 2010, 2021)
Other facies such as: chaotic slope fan facies, channel levee, mass transport facies, lowstand basin sheet sands, intraslope fans, levee overbank, channel splay, structural hyperpressuring	(Huffman and Castagna, 2001; Lu et al., 2005; Dutta et al., 2010; Shaker, 2016)

2 Method

Different databases were checked for research papers using keywords "shallow water flow", "SWF sands", "SWF zones", "shallow geohazards", "geohazard in deep-water", "geology of SWF sands", "SWF prediction", etc. Most published papers have focused on approaches to dealing with drilling problems. These studies are not investigated in this review. Several studies have been done on mechanisms, geological settings, identification criteria, and prediction of SWF sands predrilling. These kinds of studies were selected in this review. According to the objectives of this paper, different information have been extracted from these papers reviewed in section 3.

3 Results and discussion

3-1 The geological environment of SWF zones

SWF occurs in deep continental margin waters (Zhang et al., 2018). Up to now, SWF has been reported in the South Caspian Sea, the Gulf of Mexico, the Nile Delta region, east of the Mediterranean Sea in the North Sea, the East Coast of India, the Norwegian Sea, Malaysia, and North of the South China Sea (Figure. 1).

The geological conditions of this geohazard are very similar to the geological conditions of gas hydrates (Dutta et al., 2010). This geohazard occurs in environments that have tectonic uplift around and rapid subsidence. The predominant fault system of the SWF areas is the normal faults which cause rapid subsidence of the basin. As a result of rapid subsidence, the deposition rate of sediments is high in these basins, one of the requirements of the SWF-prone area.

Sand formations have been deposited during the Pleistocene low-stands (Ostermeier et al., 2002; Lu et al., 2005;

Dutta et al., 2010, 2021). These sandy sediments are found in various stratigraphic features (Table 1). The buried channels will be associated with SWF sands if these features have been overpressured. As the sea level rises, the channels are covered by fine-grained sediments. Therefore, SWF sands are quickly sealed and overpressurized due to overburden stress. These findings were also reported by Dutta et al. (2021), which categorized geological environments for SWF sands into three classes: channel sands, turbidity sands, and rotated slump blocks.

Landslides and slope failure occurrence is another possible explanation for the geological environment of SWF in the deep-water basin. Mass transport deposits (MTDs) create a topography with an erosional base and a rugose upper surface. This result is in line with those obtained by Mcgiveron and Jong (2018). As the sea level decreases, this topography is filled with sandy turbidities, resulting in semi-isolated higher permeability ponds. Also, the ponds are covered by low permeability clay as the water level rises. Mcgiveron and Jong (2018) introduced the sands inside these ponds as SWF-prone.

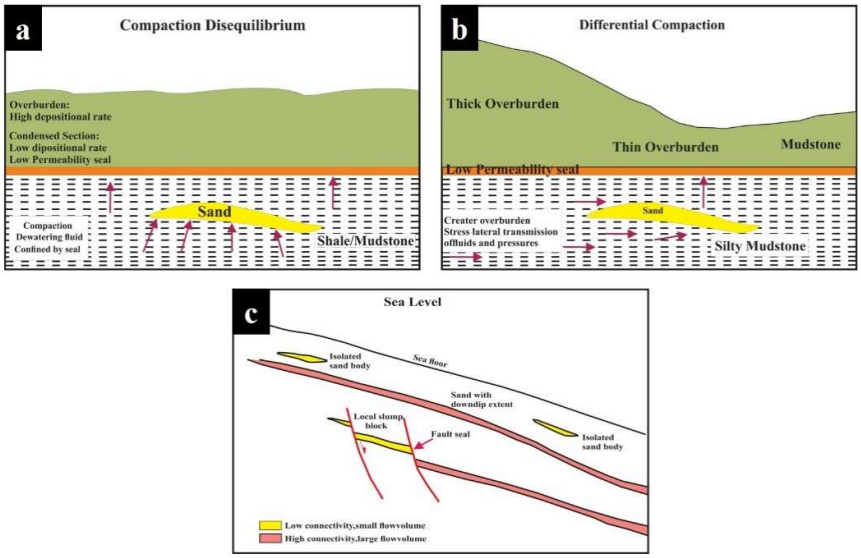

Figure 2. (a) Compaction disequilibrium (b) differential compaction (Alberty et al., 1999) (c) hydrological continuity and the ability to produce fluid can indicate the SWF sand (from Huffman and Castagna, 2001).

3-2 Mechanisms of SWF

Many studies such as Huffman and Castagna (2001), Dutta et al. (2010), McConnell et al. (2012) and Shaker (2015), point out that the SWF occurs in basins with high sedimentation rates, so the sediments are unconsolidated, the porosity, permeability and pore pressure of sediments are high, and the failure strength is low. Together these results provide important insights into essential conditions for the formation of a SWF zone:

1) Sand sediments have been deposited with a high sedimentation rate;
2) Existence of suitable shale/clay seal;
3) Existence of overpressure within the sandy zone.

The most important SWF mechanisms related to the findings include:

1) Compaction disequilibrium (Alberty et al., 1999);
2) Differential compaction (Alberty et al., 1999);
3) Structural hyperpressuring (Huffman and Castagna, 2001; Ostermeier et al., 2002; Purnomo and Ghosh, 2018).

In the compaction disequilibrium mecha-

nism, geopressure results from the deposited overburden rapidly. Therefore, this increases the pore pressure of underlying porous sediments (overpressure sands). The transmitted pressure to the SWF zone is faster than the seal, allowing water to escape. Weak grain-to-grain contact occurs in these zones due to compaction disequilibrium in SWF sands. Thus, the effective stress decreases, and therefore, the pore pressure increases. The conditions of compaction disequilibrium are shown in Figure. 2-a (Alberty et al., 1999).
In differential compaction, sandy lenses are surrounded by silty shale. A sealing layer covers the silty shale but has no contact with the sandy lens (Figure. 2-b).

Recent sediment deposits called overburden apply pressure directly onto the silty shale (not the sandy lens). This pressure is laterally transmitted to the sandy lenses and predisposes SWF (Alberty et al., 1999).

The structural hyper-pressure mechanism referred to as the "centroid effect" creates a reservoir that causes SWF. It is a condition in which the sand is on a slope or structure and has expanded regionally (Figure. 2-c). The upper part of the sand has a higher pore pressure than the surrounding shales, and this pore pressure is close to the fracture gradient.

The common denominator of all three mechanisms is that the sedimentation rate is so rapid that does not allow sediment to drain.

Seabed topography, mudflows, shallow structural features, and hydrated gas explosions are the other causes of SWF (Shaker, 2016). Expansion of sand aquifers and buoyancy effects are other factors in the formation of SWF (Dutta et al., 2010).

The magnitude of shallow water flow risk is related to seal strength, lithology, thickness, seal distribution, and buoyancy effects.

Taken together, these results suggest the flowchart in Figure. 3 about the SWF mechanisms.

3-3 Damages and drilling problems in SWF zones

Until 1998, 123 wells were hit in the Gulf of Mexico by the SWF, and 24 percent of them were damaged and unassessed. More than $ 30 million has been spent on SWF prevention and $ 137 million on reconstruction. According to the Fugro Geoservices (2000) report, 70% of all deep wells have SWF experience (Huffman and Castagna, 2001). In a well, it is estimated that 34% of the cost is spent on preventing SWF, and 66% is the cost of repairing it. The costs incurred by SWF are an essential part of deep-water exploration costs (Ren et al., 2018). This geohazard has been observed in some drilled wells in the South of the Caspian Sea (Azerbaijan and Iran).
Among the issues that these types of geohazards create in deep water include (Alberty et al., 1999; Ostermeier et al., 2002; Dutta et al., 2010, 2021):
1) Erosion around the casing shoe will cause the dilation of sands and flow into the hole and sedimentation within the ocean floor;
2) Sand washout;
3) Buckling and destruction of the casing;
4) Significant compaction due to the release of formation fluid, subsidence, and therefore the creation of large cracks within the wellhead and crater;
5) Cement failure and cracking in the surrounding wellbore due to low difference in fracture gradient and pore pressure;
6) Sinking wellhead and conductor;
7) Loss of integrity and control of the well and finally, its abandonment.
Therefore, evaluating SWF sands prior to drilling is essential in reducing drilling risks.

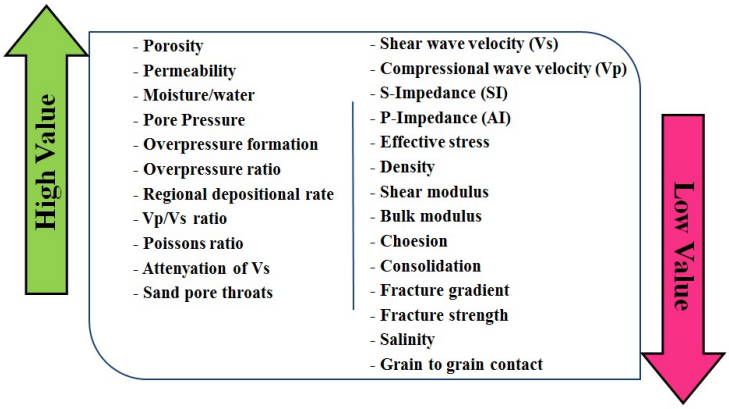

Figure 4. Quantitative and qualitative criteria for identification of SWF.

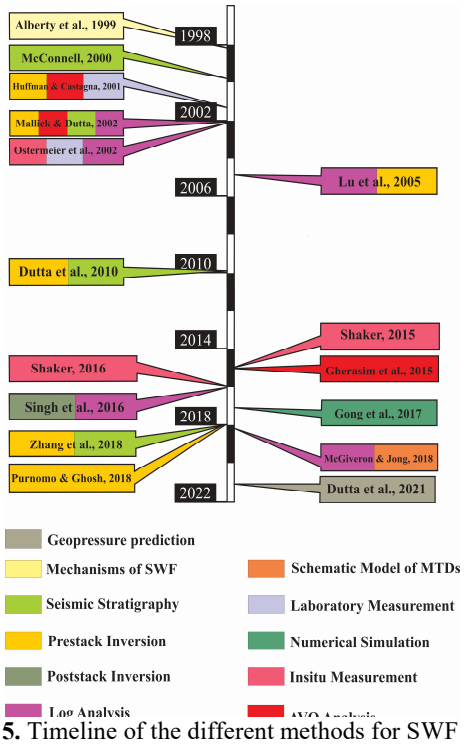

Figure 5. Timeline of the different methods for SWF studies.

Table 2. Data required for SWF evaluation

Authors	Data Types for SWF Investigation		
(Zhang et al., 2018)	Pre-stack	2D	Seismic Data
(McConnell, 2000)	Post-stack		
(Huffman and Castagna, 2001; Purnomo and Ghosh, 2018)	Multicomponent		
(Lu et al., 2005; Dutta et al., 2010; Singh et al., 2016)	Pre-stack	3D	
(McConnell, 2000; Dutta et al., 2010; Mcgiveron and Jong, 2018)	Post-stack		
(Ostermeier et al., 2002; Mcgiveron and Jong, 2018; Zhang et al., 2018)	Sonic		Log Types
(Ostermeier et al., 2002; Lu et al., 2005; Mcgiveron and Jong, 2018)	Gamma Ray		
(Ostermeier et al., 2002; Mcgiveron and Jong, 2018)	Resistivity		
(Ostermeier et al., 2002)	Density		
(Ostermeier et al., 2002)	Pressure measuring tools		In situ Measurements
(Ostermeier et al., 2002)	Geotechnical well information & Laboratory measurement		

3-4 Data and criteria for SWF evaluation

Table 2 shows the data required for SWF evaluation based on various research. Multicomponent seismic data are expensive; therefore, conventional 3D seismic data is recommended. However, these data are cost-effective and allow pre-stack inversion and quantitative velocity analysis, but signal-to-noise ratio may not be optimal and may require reprocessing. These results are inline with Dutta et al. (2021). The gamma-ray log also is used to separate sand from shale. The low value of gamma rays usually will indicate sandy sediments in which SWF zones are presented if the Vp/Vs ratios are abnormally high. The resistivity log also shows washout, which is prone to SWF problem. Dutta et al. (2021) believed that in situ measurements of elastic properties of SWF sediments have been very limited since the SWF zone is related to low velocities of sediments.

Figure. 4 and Table 3 show some criteria for identifying SWF sands. Among the mentioned parameters, Vp/Vs ratio is a key factor for identifying the SWF zone. Table 2 shows that the value of Vp/Vs ratio and Poisson's ratio are greater than 4 and 0.46, respectively. However, these values could vary in different deep-water basins.

Consistent with the literature (Huffman and Castagna, 2001; Lu et al., 2005; Purnomo and Ghosh, 2018; Wu et al., 2018), SWF sands compared to surrounding sediments are characterized by the high value of Vp/Vs ratio and Poisson's ratio. Vp/Vs increases with depth in normal compacted sands and clay layers but Vs drops in SWF sediment severely due to the weak grain-to-grain contact which results in significantly increase in Vp/Vs ratio.

Table 3. Quantitative criteria for identifying the SWF

Quality Value	Parameters		Quantity Value	Authors
High	Vp/Vs Ratio		> 9.0	(Lu et al., 2005)
			4.0-15.0	(Zhang et al., 2018)
			5.0-30.0+	(Dutta et al., 2010)
	Poisson's Ratio		0.46-0.49	(Zhang et al., 2018)
			Approaching 0.5 (0.47-0.495)	(Dutta et al., 2010)
	Pore Pressure (psi)		Above Hydrostatic	(Dutta et al., 2010)
			2000 psi	(Huffman and Castagna, 2001)
	Regional Depositional Rate (mm/yr)		> 1	(Wu et al., 2018)
	Overpressure Formation (psi or MPa)		$>$ 200 psi	(Huffman and Castagna, 2001)
			0.7–0.85 MPa	(Zhang et al., 2018)
	Overpressure Ratio (λ)		0.7-1.0	(Zhang et al., 2018)
	Porosity (%)		38-50	(Huffman and Castagna, 2001; Zhang et al., 2018)
			40-65	(Dutta et al., 2010)
Low	Shear wave velocity (Vs) (m/s)		100-700	(Dutta et al., 2010)
	Compressional wave velocity (Vp) (m/s)		1550-2000	(Dutta et al., 2010)
			1560-1900	(Zhang et al., 2018)
	S-Impedance (SI) ($gcc^{-1}ms^{-1}$)		500	(Zhang et al., 2018)
	P-Impedance (SI) ($gcc^{-1}ms^{-1}$)		2200	(Zhang et al., 2018)
	Effective stress (MPa)	0-6.0 MPa	(Zhang et al., 2018)	
		1100 psi	(Huffman and Castagna, 2001)	
	Density (gm/cc)	1.6-2.0	(Dutta et al., 2010)	

Overpressure ratio (λ) is defined as the ratio of overpressure to effective hydrostatic stress. A ratio close to 1 shows that fluid pressure is close to the overburden stress where the pore fluids are bearing the entire load (Dugan and Flemings, 2002). The value of zero is for fully drained systems.

3-5 Geophysical methods for SWF evaluation

Figure. 5 shows the timeline of SWF study methods during the past two decades. The most important methods can be summarized into three groups as follows:

1) Seismic inversion;
2) Seismic stratigraphy and attribute studies;
3) Pore pressure prediction.

3-5-1 Seismic inversion method

Inversion is a method in which a geological model is often obtained from input seismic data. The importance of seismic inversion is due to the use of various data such as seismic, well, and geological information that increase the resolution and accuracy of the model. Two typical inversion methods are:

1) Acoustic impedance inversion;
2) Simultaneous inversion.

3-5-1-1 Acoustic impedance inversion (or post-stack inversion)

The basic concept of seismic data inversion was first proposed to create impedance logs by Delas et al. (1970) and was studied by other authors such as Lindseth (1972) and Lavergne (1975). This method is also used to interpret the stratigraphic framework (Chopra and Marfurt, 2005). Geological information, including lateral changes in lithology and porosity, is enhanced by interpreting the seismic data. In this method, there are two types of input data for the inversion process. One is seismic data, and the other is the impedance model which is made by constructing a model using well logs. The seismic inversion technique is used to determine the seismic impedance. In a post-stack seismic section, the traces are modeled using the convolution of the Earth's reflectivity and bandlimited wavelet (Russell and Hampson, 2006), so the Earth's reflectivity in zero offsets is written as follows:

$$R_{0t} = \frac{AI_{i+1} - AI_i}{AI_{i+1} + AI_i} \quad ; \quad AI = \rho_i \times V_{pi}$$

where R_{0t} is the Earth's reflectivity coefficient at zero offsets. AI is the i^{th} impedance of the i^{th} layer. ρ is density and Vp is the P wave velocity.

Seismic reflection data can be inverted to P-impedance using the equations presented in Russell and Hampson (2006). The acoustic impedance seismic inversion method has improved recently. It was divided into different groups, including model-based, sparse-spike, stratigraphy, and geostatistics, which provide acceptable results (Chopra and Kuhn, 2001). Singh et al. (2016) used the post-stack inversion method to identify the SWF zone.

3-5-1-2 Simultaneous inversion (pre-stack inversion)

Simultaneous inversion extends the post-stack impedance inversion method to the pre-stack domain. In the post-stack inversion, seismic reflections are assumed to cross the boundary between two geological layers at zero degrees. In the pre-stack inversion, the angle of incidence is more significant than zero, and P wave incidents are at angle q. The amplitudes of the waves reflected and transmitted are often calculated using the Zoeppritz equation (Zoeppritz, 1919). Various pre-stack inversion methods have been used to evaluate the SWFs and gas hydrates geohazards by many researchers (Huffman and Castagna, 2001; Mallick and Dutta, 2002; Lu et al., 2005; Dai et al., 2008; Dutta et al., 2010; Forte et al., 2015; Zhang et al., 2018). In the simultaneous inversion, the common depth points (CDP) gathers are inverted to determine the P-impedance, S-

impedance, and density (Moghanloo et al., 2018). Ma (2001) used impedances as a model parameter instead of reflection coefficients and created reliable results. Ma (2001) also made changes in the equation of Fatti et al. (1994) by replacing Vs/Vp with SI/AI, so the reflection coefficient R(θ) is related to the three parameters AI, SI, and θ. The SI/AI ratio is not estimated from the impedance model but is determined from impedance model of each iteration (Fawad et al., 2020).

The pre-stack inversion is useful to the analysis of the fluid potential of reservoirs. As mentioned, the purpose of pre-stack inversion is to determine the P-impedance, S-impedance, and density (Hampson et al., 2005). Also, Vp/Vs and Poisson's ratios which are the most important parameters for SWF evaluation, are extracted from simultaneous inversion.

3-5-2 Seismic stratigraphy and seismic attributes

Interpretation of sedimentary systems provides the initial framework for studies and quantitative assessment of the drilling hazards potential (Dutta et al., 2010). 3D seismic data with the creation of horizon slice and time slice, and also seismic attributes are the best types of seismic data to review sedimentary patterns and stratigraphy (McConnell, 2000). SWF sands are the result of sedimentation at sea-level lowstand. Channels, slumps, and debris flows are the most critical seismic facies associated with the SWF geohazard. The SWF evaluation of seismic data is based on studying the seismic reflectors (seismic attributes, architecture, amplitude, etc.) and identifying these sedimentary facies (McConnell, 2000). Seismic attributes are an attractive tool for understanding the subsurface geology of seismic data (Almasgari et al., 2020). As mentioned earlier, SWF is a rapidly deposited impermeable sealing layer that covers the zones containing continuous or discrete sand deposits. The method of seismic attributes is also used to identify SWF sands and reduce ambiguities (Lu et al., 2005). For example, in younger basins, sandy channels are gaseous sands. They often have a strong amplitude that is easily identified by the sweetness attribute, which is useful for visualizing stratigraphic units such as channels and slumps (Ghosh et al., 2010; Dutta et al., 2021). Mud-filled channels have weak amplitudes, and channel boundaries are identified by relative amplitude changes (Almasgari et al., 2020). SWF sands are often identified by comparing the attributes between the offset wells and the planned well (Alberty et al., 1999). Table 4 shows the relevant attributes to identify SWF sands. Among the mentioned attributes, Vp/Vs is crucial for identifying SWF sands. A high value of Vp/Vs represents the SWF zones. Some researchers (Lu et al., 2005; Dutta et al., 2010; Zhang et al., 2018) believe that low S-Impedance (SI) is the best attribute to identify SWF potential.

3-5-3 Pressure prediction in SWF zones

In most deep sedimentary formations, pore pressures are overpressured and also are greater than hydrostatic pressure (Zhang, 2011). Overpressure is often created by hydrostatic pressure, compaction disequilibrium, aqua thermal expansion, mineral transformation, and tectonic compression (Gutierrez et al., 2006).

The Biot and Terzaghi effective stress law is the main theory for predicting pore pressure (Biot, 1941; Terzaghi et al., 1996). Predicting pore pressure is one of the most challenging tasks in identifying a SWF zone at 200 feet below the seabed (Alberty et al., 1999). Generally, pore pressure and fracture pressure play a significant role in well design and reservoir modeling (Mahetaji et al., 2020).

Many researchers (Alberty et al., 1999; Huffman and Castagna, 2001; Ostermeier

et al., 2002; Dutta et al., 2010; Singh et al., 2016; Zhang et al., 2018) have used different methods for measuring and predicting the pore pressure in SWF zones. In various studies, rock physics analysis has shown that the SWF zone has very low effective pressure and extremely high pore pressure (Dutta et al., 2021). Furthermore, the pressure value in these sands is close to the fracture gradient (fracture gradient is the maximum weight of the mud and is a crucial parameter in drilling planning) (Purnomo and Ghosh, 2018).

Table 4. Related attributes to identify SWF sands

Authors	Location of SWF	Attribute Type
(Huffman and Castagna, 2001) (Lu et al., 2005) (Zhang et al., 2018) (Purnomo and Ghosh, 2018)	Gulf of Mexico (GOM) Gulf of Mexico (GOM) Northern South China Sea Offshore Malaysia (Malay Basin)	Vp/Vs
(Lu et al., 2005) (Singh et al., 2016) (Zhang et al., 2018)	Gulf of Mexico (GOM) Krishna Godavari basin on the east coast of India Northern South China Sea	AI (P-Impedance)
(Zhang et al., 2018) (Lu et al., 2005)	Northern South China Sea Gulf of Mexico (GOM)	SI (S-Impedance)
(Shen et al., 2018)	Northern South China Sea	ground-penetrating radar (GPR) attributes Weighted average frequency Sweetness

SWF problems are mainly the result of a narrow window between the pore pressure and the fracture gradient in SWF sands (Ostermeier et al., 2002). Direct measurements of formation pressure near the surface are not accurate in SWF zones. Pressure determination in these zones is based on mud weight, PWD logs, and daily reports (Ostermeier et al., 2002). Logging while drilling (LWD), measurement while drilling (MWD), drilling parameters, and mud logging data are mainly used to predict the pore pressure during drilling. The change in pore pressure is often measured using sonic, resistivity, porosity, and density logs. Pore pressure effects in these logs are well defined due to the relationship between porosity, density and also, electrical and acoustic properties (Chopra and Huffman, 2006). Moreover, the calculation of the pore pressure of the formation is often done by knowing the porosity of the formation, and therefore, the normal porosity trend (from well logs).

Quantitative seismic methods that include effective stress and pore pressure determination, identify the drilling risk within the SWF zone and calculate the degree of risk (Dutta et al., 2010). Density resulting from seismic inversion can be used to calculate the overpressure (Dutta et al., 2010). Many researchers (Matthews and Kelly, 1967; Eaton, 1975; Yan et al., 2012) have presented the pore pressure equations of seismic data.

Another method to detect the SWF zone is overpressure prediction in this zone qualitatively. Alberty et al. (1999) and McConnell (2000) believed that the first continuous and sealing layer above the shallow sand zone is identified from seismic data (sealing layers are very bright, medium to high amplitude, and have regional continuity). Sealing assessment in seismic data is especially important to detect the presence or absence of overpressure. For instance, acoustic blanking or other amplitude phenomena within the sealing layer suggest that the fractures are local in scale and transmit overpressure. In contrast, if the sealing layer near the proposed well is fractured, the sand zone below the sealing layer does not have an overpressure (McConnell, 2000). Also, if the sedimentation rate within the shallow zone is more than 500 feet per million years, the sand under this sealing layer is under pressure. If the sedimentation rate

of the shallow zone is smaller than 500 feet per million years, the shallow sands do not have significant pressure. A method to identify geopressure using seismic data is to organize isopach maps of the overburden pressure that covers the clay/shale sealing layer. Thus, the areas with geopressure potential are identified qualitatively (Alberty et al., 1999). About the overburden assessment, if there is evidence of rapid deposition (such as slumps and other rapid mass movements) at the well site, it indicates overpressure within the SWF zone.

4 A case study: evaluation of SWF in the South Caspian Basin

4-1 Geology of the South Caspian Basin

The South Caspian Basin has large hydrocarbon reservoirs within the Early Pliocene production series (Vincent et al., 2010). This sub-basin extends from the heights of the Alborz Mountains to the deepest part of the Caspian Sea (Lahijani et al., 2019). The maximum water depth of the South Caspian reaches 1025 meters (Lahijani et al., 2019). The average precipitation of sediments from east to west of the South Caspian Sea increases from less than 150 mm/y to about 2000 mm/y (Leroy et al., 2011). Characteristics of the South Caspian include high deposition rate of sediments, sediment thickness above 20 km, low sediment density, low geothermal gradient, and high-pressure gradient (Smith-Rouch, 2006), which give the conditions for the formation of SWF zone.

An important issue about the South Caspian Basin is the existence of channels in this basin. As mentioned earlier, buried shallow channels are the most facies for creating the SWF zone. These channels within the South Caspian Sea are the most critical geohazards with overpressure and saturation of water or gas, which causes many problems in drilling operations (Karbalali et al., 2018). Therefore, the necessity to review these channels in identifying SWF within the South Caspian is quite apparent and must be identified before drilling operations. The maximum of SCB tectonic subsidence occurred within the Pliocene-Quaternary. The value of tectonic subsidence during Pliocene-Quaternary reaches 2 km, with a very high subsidence rate (Brunet et al., 1997). The evolution of SCB subsidence consists of two stages. The first stage is related to the extension and cooling from the Jurassic to the Pliocene. The second stage is the rapid and short subsidence phase during the Pliocene to Quaternary times. This subsidence coincides with the uplift of the Caucasus Mountains, Kopeh Dagh Alborz (Brunet et al., 2003). Due to the rapid sedimentation, the sediments are buried under compaction, allowing the event of mud volcano (Brunet et al., 2007) and the formation of SWF zones. South Caspian sediments are unconsolidated (Narimanov, 1993) and their average density ρ_{sd} is about 2500 kg/m^3 (Brunet et al., 2003). The subsidence value of SCB is $>$ 2.0 km/Ma and seafloor tempreture and geothermal gradients are 5.8-6.2° C, and 11-17° C, respectively (Diaconescu et al., 2001). Therefore, this condition may be a suitable environment for the formation of SWF sands and gas hydrate. In the Quaternary, the sedimentation rate increased only within the Azerbaijan part of the SCB and reached 2.4 km/My. In the upper Pliocene, the sedimentation rate decreased after its maximum value (Nadirov et al., 1997). Aging results also show sedimentation rates between 1.4 to 2.45 mm/yr within this basin (Karbassi and Amirnezhad, 2004).

Due to the tectonic setting, the sedimentation rate is rapid in the subsidence basin. In that case, it will cause a considerable thickness of sediments to be deposited during a short time. Increasing the overburden will cause overpressure for-

mations, which may be a dangerous parameter in exploratory drilling. According to previous studies in other parts of the world, if the sedimentation rate is more than 150 meters per million years, shallow water flow (SWF) will be likely. However, the sedimentation rate in the South Caspian has been more than this rate. The SWF geohazard occurs in overpressure and unconsolidated sands in the South Caspian Sea. These sandy sediments were deposited less than half a million years ago. Due to the geological conditions and sedimentation history of the Caspian Sea, there is a possibility of this problem in the South Caspian Sea. Mousavi-Roubakhsh (2001) believed that the South Caspian Basin is one of the regions with abnormal formation pressure, such as the Gulf of Mexico. Future exploration plans of this exploration basin should be adjusted based on overpressure basins. Therefore, according to the previous studies in SCB and the present review study, the South Caspian Basin has all the standard quality criteria introduced in section 3 of this paper and has unique conditions for the formation of SWF zones.

4-2 Seismic and log data in the South Caspian Sea

The seismic data used in this study is 3D post-stack seismic data with SEG polarity. The 3D seismic data was acquired with a bin spacing of 12.5 m (xline direction) × 25 m (inline direction) and a 4 m vertical sampling interval. The high-frequency content in seismic data is about 57 Hz, with the dominant frequency of about 40 Hz. The reflection quality of post-stack 3D seismic data is suitable for the interpretation of faults, horizons, and stratigraphic features such as channels. Well-log data includs P-wave and density log. Density log is not available in the SCB, so the Gardner equation was applied to create it.

4-3 Method of SWF evaluation in the South Caspian Sea

Seismic attributes specified as any calculation on seismic data that quantify some features of structural and depositional environment (Chopra and Marfurt, 2005), thereby could identify some properties of interest. In this paper, possible locations of channels and SWF zones have been identified by sweetness on the post-stack 3D seismic data.

Seismic inversion is usually applied to estimate the earth model (Russell, 1988). Inversion analysis has been done to select the different optimization parameters at well location (Russell and Hampson, 2006). The synthetic seismogram was created by convolving the reflectivity and wavelet derived from density and acoustic well logs and real seismic data. Nanda (2016) recommended to extract the seismic wavelet statistically. The generated seismogram was used for the well-seismic tie in post-stack seismic inversion to determine the two-way travel-time and the depth of the target zone. The tie between the seismic data and synthetic data is relatively good at the well location in the zone of interest. Incorrect tying well logs to the seismic data can lead to unreliable models that reduce the confidence of inversion results. Then, the initial low-frequency model (LFM) was applied by interpolating corresponding well log data (P-wave and density) along with seismic data. The initial model was updated until synthetic data approximated seismic data to obtain the inverted acoustic impedance.

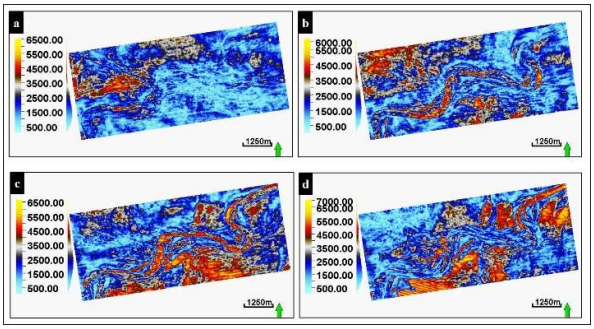

Figure 6. Different extracted maps of sweetness attribute below H1. (a) 40 ms (b) 50 ms (c) 60 ms (d) 70 ms.

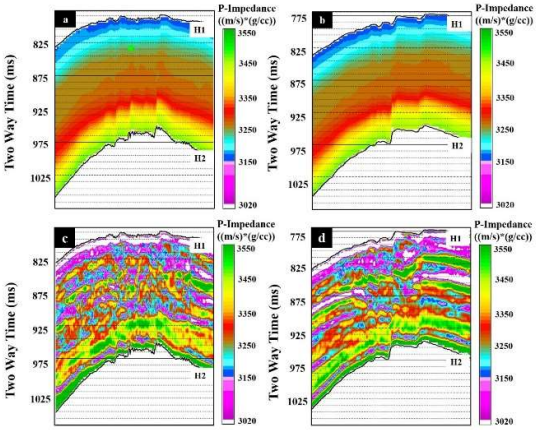

Figure 7. (a,b) The initial low frequency model of the P-impedance along inline and xline, respectively. (c,d) P-impedance sections after post-stack seismic inversion along inline and xline, respectively. Note: P-impedance is decreased in SWF zones.

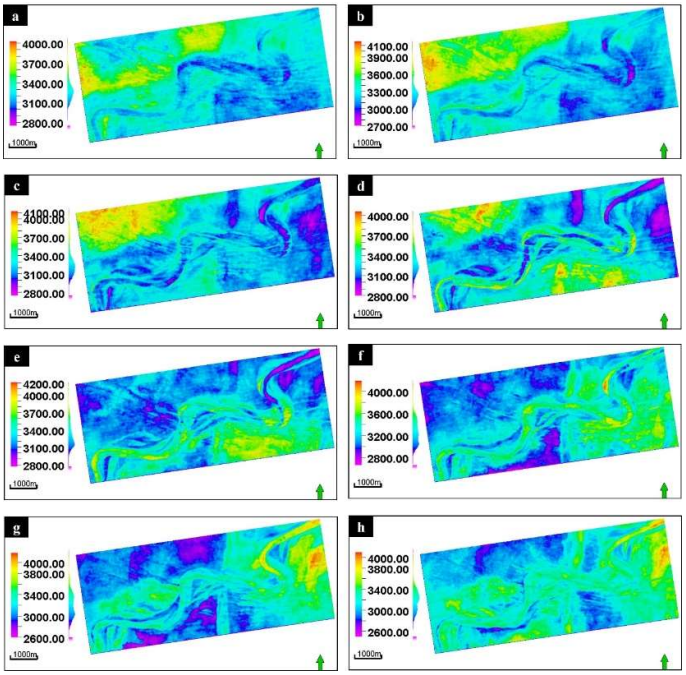

Figure 8. Extracted maps of P-impedance (AI) from post-stack inversion below H3 from post-stack inversion (a) 40 ms (b) 45 ms (c) 50 ms (d) 55 ms (e) 60 ms (f) 65 ms (g) 70 ms (h) 75 ms. Note: a significant SWF sand zone could be seen at 45 ms to 60 ms below H1 in the central and eastern parts of the channel but from 60 ms to 70 ms below H1, no SWF problem is observed.

Two seismic horizons (H1 and H2) were interpreted at a few distances from the top and base of the channel zone.

4-4 Results and discussion of SWF evaluation in the South Caspian Sea

Figure. **Error! Reference source not found.**6 displays different extracted maps of the sweetness attribute below H1. Sandy channel has been observed with hot color in 50 ms to 70 ms below H1. Therefore, the channel is located between H1 (800 ms) and H2 (1050 ms), and the target window is determined for post-stack seismic inversion in this range.

In this study, the post-stack seismic inversion method is model-based with hard constraint 100%. Figure. 7 shows the initial model along inline and xline.

According to the initial model (Figures. 7-a , 7-b) and the selected inversion method, an appropriate match between real and synthetic data has been derived from inversion with minimum misfit error estimates (Figure. **Error! Reference source not found.**9).

P-impedance sections (along inline, xline) of post-stack inversion have been shown in the SWF zone (Figures. 7-c , 7-d). The most interesting aspect of Figures. 7-c and 7-d is that low P-impedance layers (AI<3150((m/s).(g/cc)) which are surrounded by higher impedance layers, are the most likely parts of the section for creating SWF. That is related to the interpreted channel in Section 4-4-1. In order to assess the location of the SWF sands in this channel more accurately, Figure. 8 shows map views of P-impedance between the H1 and H2 horizons. In these map views, from 45 ms to 60 ms below horizon H1, we predict a significant SWF sand problem in the central and eastern parts of the channel. Especially, for 55 ms below horizon H1, the full channel involves SWF problem. However, we have not been observed any SWF problem from 60 ms to 70 ms below H1 by post-stack inversion method.

Low impedance zones (AI<3150((m/s).(g/cc)) in Figures. 7-c and 7-d are consistent with low impedance zones in the map views of the channel. Results from previous studies by Lu et al. (2005) and Zhang et al. (2018) pointed out that the channels are the most important facies for SWF problem.

5 Conclusion

This review study introduces the problem of shallow water flow (SWF) and its consequences as a geohazard in hydrocarbon exploration operations within the deep-water basin. It refers to the South Caspian Basin as one of the SWF-prone deep-water basins. The main points can be summarized as follows:

- Shallow water flow (SWF) is reported in different deep-water basins at depths of 100 to 1000 meters below the seabed in continental margin environments;
- From a geological point of view, the basins with rapid subsidence and high sedimentation rates are ideal for the SWF problem. In SWF-prone environments, sands are mainly related to Pleistocene and deposited in the channel, slump, debris flow, turbidity sands, and chaotic

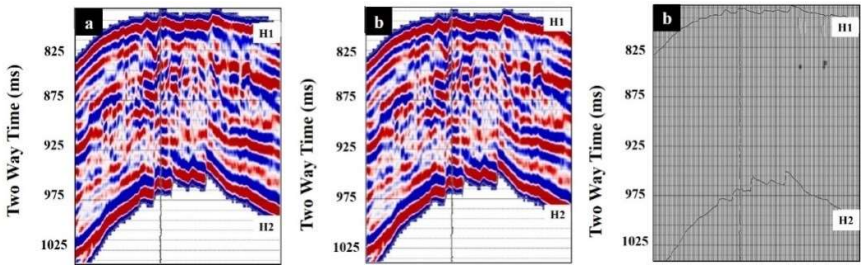

Figure 9. Real vs. synthetic data and inconvenient error derived from the inversion.

zone in the lowstand system tract;
- The main reason for SWF sands eruption is overpressure water in the sandy zone under the sealing layer. Generally, the three main mechanisms which are important mechanisms for creating SWF are: compaction disequilibrium, differential compaction and structural hyperpressuring;
- SWF causes buckling of the casing, washout of the sand zone, loss of well integrity, and in some cases, destruction of the platform and abandonment of the well;
- Many quantitative and qualitative criteria have been introduced to identify SWF sands. The foremost important are: Vp/Vs ratio, Poisson's ratio, formation overpressure, fracture gradient, under compaction, unconsolidation sediments, P-impedance, and S-impedance;
- Many methods for studying SWF will be selected consistent with the type of data available (seismic data, well logs, and in situ measurements). These methods include the seismic stratigraphic method, attributes studies, pre-stack and post-stack inversion, and pressure prediction in the SWF zone;
- As one of the world's largest deep-water basins in hydrocarbon exploration, the South Caspian Basin is prone to SWF occurrence in its various parts. This basin has suitable qualitative and quantitative criteria for the SWF problem.

The findings of this study have a number of important implications for drilling risk and development plans in deep-water basins.

Acknowledgments

The paper has been extracted from the Ferdowsi University of Mashhad research project with the approval code 3.46927. Also, it has been done in collaboration with the Khazar Exploration and Production Company (KEPCO) with approval code 97-202 as an Industrial Research Project.

References

Alberty, M. W., Hafle, M. E., Mingle, J. C., and Byrd, T. M., 1999, Mechanisms of shallow waterflows and drilling practices for intervention: SPE Drilling and Completion, **14**, 123–129, https://doi.org/10.2118/56868-PA.

Ali, H. K., Qayyum, F., de Groot, P., and Javaherian, A., 2018, Shallow geohazard channel identification based on novel seismic interpretation techniques in South Caspian Sea: 80th EAGE Conference and Exhibition, https://doi.org/10.3997/2214-4609.201801370.

Almasgari, A. A., Elsaadany, M., Latiff, A. H. A., et al., 2020, Application of seismic attributes to delineate the geological features of the Malay Basin: Bulletin of Geological Society of America, Malaysia, **69**, 97–110, https://doi.org/10.7186/bgsm69202009.

Biot, M. A., 1941, General theory of three-dimensional consolidation: Journal of Applied Physics, **12**, 155–164, https://doi.org/10.1063/1.1712886.

Brunet, F. F., Korotaev, M. V., Ershov, A. V., and Nikishin, A. M., 2003, The South Caspian Basin: A review of its evolution from subsidence modelling: Sedimentary Geology, **156**, 119–148, https://doi.org/10.1016/S0037-0738(02)00285-3.

Brunet, M. F., Rebetsky, Y. L., and Nikitina, Y. S., 1997, First steps of modelling in the South Caspian Sea: Peri-Tethys Program, Annual Meeting, Rabat, Morocco, 1997-June, 25–26.

Chopra, S., and Huffman, A. R., 2006, Velocity determination for pore-pressure prediction: The Leading Edge, **25**, 1502, https://doi.org/10.1190/1.2405336.

Chopra, S., and Kuhn, O., 2001, Seismic inversion: CSEG Recorder, **26**, 10–14.

Chopra, S., and Marfurt, K. J., 2005, Seismic attributes - A historical perspective: Geophysics, **70**,

https://doi.org/10.1190/1.2098670.

Dai, J., Banik, N., Gillespie, D., and Dutta, N., 2008, Exploration for gas hydrates in the deepwater, Northern Gulf of Mexico: Part II, Model validation by drilling: Marine and Petroleum Geology, **25**, 845–859, https://doi.org/10.1016/j.marpetgeo.2008.02.005.

Delas, G., Beauchomp, J. B., De Lombares, G., Fourmann, J. M., and Postic, A., 1970, An example of practical velocity determinations from seismic traces: 32nd EAEG Meeting, Edinburgh.

Diaconescu, C. C., Kieckhefer, R. M., and Knapp, J. H., 2001, Geophysical evidence for gas hydrates in the deep water of the South Caspian Basin, Azerbaijan: Marine and Petroleum Geology, **18**, 209–221.

Dugan, B., and Flemings, P. B., 2002, Fluid flow and stability of the US continental slope offshore: Geofluids, **2**(2), 137–146.

Dutta, N. C., Bachrach, R., and Mukerji, T., 2021, Quantitative Analysis of Geopressure for Geoscientists and Engineers: Cambridge University Press.

Dutta, N. C., Utech, R. W., and Shelander, D., 2010, Role of 3D seismic for quantitative shallow hazard assessment in deep water sediments: The Leading Edge, **29**(8), 930–942.

Eaton, B. A., 1975, The equation for geopressure prediction from well logs: Society Petroleum Engineering - Fall Meeting Society Petroleum Engineering, AIME, FM 1975, https://doi.org/10.2523/5544-ms.

Fatti, J. L., Smith, G. C., Vail, P. J., Strauss, P. J., and Levitt, P. R., 1994, Detection of gas in sandstone reservoirs using AVO analysis: a 3-D seismic case history using the Geostack technique: Geophysics, **59**, 1362–1376, https://doi.org/10.1190/1.1443695.

Fawad, M., Hansen, J. A., and Mondol, N. H., 2020, Seismic-fluid detection - a review: Earth-Science Reviews, **210**, 103347, https://doi.org/10.1016/j.earscirev.2020.103347.

Forte, A. M., Sumner, D. Y., Cowgill, E., et al., 2015, Late Miocene to Pliocene stratigraphy of the Kura basin, a subbasin of the South Caspian Basin: Implications for the diachroneity of stage boundaries: Basin Research, **27**, 247–271, https://doi.org/10.1111/bre.12069.

Fugro Geoservices, I., 2000, Shallow-water-flow assessment / Proposed Wellsites A and B / Redhawk Prospect / Garden Banks Block 877 / Gulf of Mexico.Report.

Gherasim, M., Viceer, S., Brusova, O., et al., 2015, Application of an integrated workflow for shallow-hazard characterization using 3D high-resolution survey offshore Azerbaijan: The Leading Edge, **34**, 390–396, https://doi.org/10.1190/tle34040390.1.

Ghosh, D. P., Ibrahim, N. A., Viratno, B., and Mohamad, H., 2010, Seismic attributes adding a new dimension to prospect evaluation and geomorphology identification in the Malay and adjacent basins: Society of Exploration Geophysics. Int. Expo. 80th Annual Meeting, SEG 2010, 1307–1311, https://doi.org/10.1190/1.3513083.

Gutierrez, M. A., Braunsdorf, N. R., and Couzens, B. A., 2006, Calibration and ranking of pore-pressure prediction models, The Leading Edge (Tulsa, OK), **25**, 1516–1523, https://doi.org/10.1190/1.2405337.

Hampson, D. P., Russell, B. H., and Bankhead, B., 2005, Simultaneous inversion of pre-stack seismic data: Society of Exploration Geophysics, 75th SEG Int. Expo. Annual Meeting, SEG 2005, 1633–1637, https://doi.org/10.1190/1.2148008.

Huffman, A. R., and Castagna, J. P., 2001, The petrophysical basis for shallow-water flow prediction using multicomponent seismic data: The Leading Edge, **20**, 1030–1052, https://doi.org/10.1190/1.1487308.

Karbassi, A. R., and Amirnezhad, R., 2004, Geochemistry of heavy metals and sedimentation rate in a bay adjacent to the Caspian Sea: International Journal of Environment Science and Technology, **1**, 191–198.

Lahijani, H. A. K., Abbasian, H., Naderi Beni, A., et al., 2019, Sediment distribution pattern of the South Caspian Sea: Possible hydroclimatic implications: Canadian Journal Earth Sciences, **56**, 637–653, https://doi.org/10.1139/cjes-2017-0239.

Lavergne, M., 1975, Pseudo-diagraphies de vitesse en offshore profond: Geophysical Prospecting, **23**, 695–711.

Leroy, S. A. G., Lahijani, H. A. K., Djamali, M., et al., 2011, Late Little Ice Age palaeoenvironmental records from the Anzali and Amirkola Lagoons (South Caspian Sea): Vegetation and sea level changes: Palaeogeography, Palaeoclimatology, Palaeoecology, **302**, 415–434, https://doi.org/10.1016/j.palaeo.2011.02.002.

Lindseth, R. O., 1972, Approximation of acoustic logs from seismic traces: Journal of Canadian Well Logging Society, **5**, 13–26.

Lu, S., McMechan, G. A., and Liaw, A., 2005, Identification of shallow-water-flow sands by Vp/Vs inversion of conventional 3D seismic data: Geophysics, **70**, 29–37, https://doi.org/10.1190/1.2052470.

Ma, X. Q., 2001, Global joint inversion for the estimation of acoustic and shear impedances from AVO derived P- and S-wave reflectivity data: First Break, **19**, 557–566, https://doi.org/10.1046/j.1365-2397.2001.00211.x.

Mahetaji, M., Brahma, J., and Sircar, A., 2020, Pre-drill pore pressure prediction and safe well design on the top of Tulamura anticline, Tripura, India: a comparative study: Journal of Petroleum Exploration and Production Technology, **10**, 1021–1049, https://doi.org/10.1007/s13202-019-00816-0.

Mallick, S., and Dutta, N. C., 2002, Shallow water flow prediction using prestack waveform inversion of conventional 3D seismic data and rock modeling: The Leading Edge (Tulsa, OK), **21**, 675–680, https://doi.org/10.1190/1.1497323.

Matthews, W. R., and Kelly, J., 1967, How to predict formation pressure and fracture gradient: Oil and Gas Journal, **65**, 92–1066.

McConnell, D. R., 2000, Optimizing deep-water well locations to reduce the risk of shallow-water-flow using high-resolution 2D and 3D seismic data: Proceeding of Annual Offshore Technology. Conference, **1**, 87–97, https://doi.org/10.4043/11973-ms.

McConnell, D. R., Zhang, Z., and Boswell, R., 2012, Review of progress in evaluating gas hydrate drilling hazards: Marine and Petroleum Geology, **34**, 209–223, https://doi.org/10.1016/j.marpetgeo.2012.02.010.

Mcgiveron, S., and Jong, J., 2018, A case study and model of shallow water flow (SWF) from Sabah deep-water drilling operations, offshore Malaysia: Warta Geologi, **44**, 39–47.

Moghanloo, H. G., Riahi, M. A., and Bagheri, M., 2018, Application of simultaneous prestack inversion in reservoir facies identification: Journal of Geophysics and Engineering, **15**, 1376–1388, https://doi.org/10.1088/1742-2140/aab249.

Mousavi-Roubakhsh, M., 2001, Caspian

Sea Geology (in persian): Geological Survey of Iran.

Nadirov, R. S., Bagirov, E., Tagiyev, M., and Lerche, I., 1997, Flexural plate subsidence, sedimentation rates, and structural development of the super-deep South Caspian Basin: Marine and Petroleum Geology, **14**, 383–400, https://doi.org/10.1016/S0264-8172(96)00054-2.

Narimanov, A. A., 1993, Petroleum Systems Of South Caspian Basins: Norwegian Petroleum Society.

Ostermeier, R. M., Pelletier, J. H., Winker, C. D., et al., 2002, Dealing with shallow-water flow in the deepwater Gulf of Mexico: The Leading Edge, **21**, 660–668, https://doi.org/10.1190/1.1497320.

Purnomo, E. W., and Ghosh, D. P., 2018, Identifying shallow water flow in offshore Malaysia using multicomponent data and FWI approach: Offshore Technology Conference, Asia 2018, OTCA 2018, 1–10, https://doi.org/10.4043/28276-ms.

Ren, S., Liu, Y., Gong, Z., Yuan, Y., Yu, L., Wang, Y., Xu, Y., and Deng, J., 2018, Numerical simulation of water and sand blowouts when penetrating through shallow water flow formations in deep water drilling: Journal of Ocean University of China, **17**, 17–24, https://doi.org/10.1007/s11802-018-3454-5.

Russell, B., and Hampson, D., 2006, the old and the new in seismic inversion: CSEG Recorder, **31**, 1–12.

Russell, B. H., 1988, Introduction to Seismic Inversion Methods, Volume 2 of Course notes series: Society of Exploration Geophysicists, https://doi.org/10.1190/1.9781560802303.

Shaker, S. S., 2015, A new perspective on shallow water flow (SWF) prediction and the prevention of sinking well-heads in deep-water settings: CSEG Recorder, **40**, 34–40.

Shaker, S. S., 2016, Causes and deterrent of SWF in deep water of Mississippi prodelta areas: The Leading Edge, **35**, 330–335, https://doi.org/10.1190/tle35040330.1.

Shen, Y., Tang, T., Zuo, R., Zhang, Z., and Wang, Y., 2018, Identification of shallow water flow using multicomponent seismic and GPR attributes in the deep-water basin of the northern South China Sea: Indian Journal of Geo-Marine Science, **47**, 1742–1748.

Singh, K., Dalei, S. N., and Bhardwaj, A., 2016, De-risking shallow hazards through pore pressure prediction and special studies - A case study from KG-offshore basin: Proceeding of Indian National Science Academy, **82**, 935–943, https://doi.org/10.16943/ptinsa/2016/48494.

Smith-Rouch, L. S., 2006, Oligocene-Miocene Maykop/Diatom total petroleum system of the South Caspian Basin Province, Azerbaijan, Iran, and Turkmenistan: U.S. Geology Survey Bulletin, 2201-I, 27.

Terzaghi, K., Peck, R. B., and Mesri, G., 1996. Mechanics in Engineering Practice, 3rd Edition: John Wiley & Sons.

Vincent, S. J., Davies, C. E., Richards, K., and Aliyeva, E., 2010, Contrasting Pliocene fluvial depositional systems within the rapidly subsiding South Caspian Basin; a case study of the palaeo-Volga and palaeo-Kura river systems in the Surakhany Suite, Upper Productive Series, onshore Azerbaijan: Marine and Petroleum Geology, **27**, 2079–2106, https://doi.org/10.1016/j.marpetgeo.2010.09.007.

Wu, S., Wang, D., and Völker, D., 2018, Deep-sea geohazards in the South China Sea: Journal of Ocean University of China, **17**, 1–7,

https://doi.org/10.1007/s11802-018-3490-1.

Yan, F., Han, D. H., and Ren, K., 2012, A new model for pore pressure prediction: Society of Exploration Geophysics, Int. Expo. 82nd Annual Meeting, SEG 2012, 2041–2045, https://doi.org/10.1190/segam2012-1499.1.

Zhang, J., 2011, Pore pressure prediction from well logs: Methods, modifications, and new approaches: Earth-Science Reviews, **108**, 50–63, https://doi.org/10.1016/j.earscirev.2011.06.001.

Zhang, X., Sun, Y., Wu, S., and Dong, D., 2018, Geophysical signature of the shallow water flow in the deepwater basin of the Northern South China Sea: Journal of Ocean, University of China, **17**, 791–798, https://doi.org/10.1007/s11802-018-3487-9.

Zoeppritz, K., 1919, VII b. Über Reflexion und Durchgang seismischer Wellen durch Unstetigkeitsflächen. Nachrichten von der Gesellschaft der Wissenschaften zu Göttingen; Math. Klasse, 66–84.